
PHASE
TRANSITIONS

Thermal, Optical, and Dielectric Properties of Fluoride Rb_2TaF_7

E. I. Pogorel'tsev^{a, b*}, S. V. Mel'nikova^a, A. V. Kartashev^{a, c}, M. V. Gorev^{a, b},
I. N. Flerov^{a, b}, and N. M. Laptash^d

^a Kirensky Institute of Physics, Federal Research Center, Siberian Branch, Russian Academy of Sciences,
Krasnoyarsk, 660036 Russia

^b Siberian Federal University, Krasnoyarsk, 660041 Russia

^c Krasnoyarsk State Pedagogical University, 660060 Russia

^d Institute of Chemistry, Far East Branch, Russian Academy of Sciences, Vladivostok, 690022 Russia

*e-mail: pepel@iph.krasn.ru

Received September 26, 2016; in final form, October 19, 2016

Abstract—The thermal, optical, and dielectric properties of fluoride Rb_2TaF_7 were investigated. It was observed that the variation in chemical pressure in fluorides $A_2^+\text{TaF}_7$ caused by the cation substitution of rubidium for ammonium does not affect the ferroelastic nature of structural distortions, but leads to stabilization of the high- and low-temperature phases and enhancement of birefringence. The entropy of the phase transition $P4/nmm \leftrightarrow Cmma$ is typical of the shift transformations, which is consistent with a model of the initial and distorted phase structures. The anisotropy of chemical pressure causes the change of signs of the anomalous strain and baric coefficient dT/dp of Rb_2TaF_7 as compared with the values for its ammonium analog.

DOI: 10.1134/S1063783417050250

1. INTRODUCTION

Among the variety of inorganic fluorides and oxifluorides are the compounds with diverse structural modifications and the related various functional properties and effects that find technological applications in energy generation and storage, photonics, microelectronics, etc. [1, 2]. The applied physical properties are, as a rule, those working at room temperature and atmospheric pressure. Therefore, until recently, the main direction in studying inorganic fluorine-containing materials has been related to the synthesis of new compounds and their structural characterization. However, it is well-known that the physical properties can anomalously change at the structural transformations resulting from phase transitions that occur upon variation in temperature, pressure, and electric or magnetic fields or in the chemical pressure under the action of the cation/anion substitutions [3, 4]. At present, one of the priority directions is searching for the ways of purposeful variation of the chemical composition, structure, and physical properties of materials, including fluorine-containing ones. One should be aware that the formation of the structure, its potential transformation, and physical properties are strongly affected by the composition and shape of one of the main structural elements of the crystals, specifically, fluorine and fluorine-oxygen polyhedra $[\text{MeX}_n]$, where Me is the central atom, X is O or F, and $n = 4$ –

9 [1–4]. The polyhedra with $n = 4$ and 5 are rarely met. The most widespread structural elements are $[\text{MeX}_6]$, $[\text{MeX}_7]$, $[\text{MeX}_8]$, and $[\text{MeX}_9]$ [2]. The phase transitions in fluorides and oxifluorides with octahedral anions are the best studied [3–5]. On the other hand, of undoubted interest as central Me atoms are the metals that, depending on valence, can form polyhedra of different configurations with the fluorine and fluorine-oxygen ligands X . Among these metals are Zr, Hf, Nb, and Ta, which can form six-, seven-, and eight-coordinate anion polyhedra. Despite a great number of works devoted to the synthesis and investigations of such compounds [6–15], the effect of structural features on the thermodynamic stability of crystal phases and their physical properties has not been systematically studied.

The measurements of specific heat, thermal expansion, optical twinning, birefringence, and permittivity of fluoride Rb_2TaF_7 performed in this work continue the study of phase transitions in the $A_2\text{MeF}_7$ compounds with the seven-coordinate anion polyhedron [7, 15, 16]. The room-temperature crystal lattice symmetry of these fluorides depends on the ionic radius of a univalent cation and is tetragonal (sp. gr. $P4/nmm$, $Z = 2$) for $A = \text{Rb}$ and NH_4 [15, 16] and monoclinic (sp. gr. $P2_1/c$, $Z = 4$) for $A = \text{K}$ [7]. The seven-coordinate anion polyhedron $[\text{MeFe}_7]$ has a polar rhombic symmetry and represents a monocapped trigonal

prism. There are no data on the thermodynamic stability of the $P2_1/c$ phase in the K_2TaF_7 crystal. The data about one structural transformation in Rb_2TaF_7 near 145 K and symmetry of the initial ($P4/nmm$) and distorted ($Cmma$, $Z = 4$) phases were reported in [15]. Two sequential structural transformations $G_1(P4/nmm) \leftrightarrow G_2(Pmmn) \leftrightarrow G_3$ (tetragonal phase) in the ammonium compound were found and thoroughly investigated in [16]. Thus, the cation substitution $K \rightarrow Tb \rightarrow NH_4$ significantly affects the symmetry of A_2MeF_7 crystals and sequence of the phase transitions. Therefore, it is interesting to study the physical properties of fluoride Rb_2TaF_7 in order to establish the nature and mechanism of structural distortions.

2. EXPERIMENTAL

In this study, we investigated the Rb_2TaF_7 crystals whose structure and synthesis technique were described in [15].

The calorimetry investigations involved two stages. At the first stage, we sought for phase transitions in Rb_2TaF_7 in a wider temperature range than in [15], where the reversible phase transition $P4/nmm \leftrightarrow Cmma$ was observed at about 145 K. The measurements were performed using a DSM-10M differential scanning microcalorimeter on a sample with a mass of ~ 0.1 g at temperatures from 100 to 400 K in the heating and cooling modes at a rate of 8 K min^{-1} . The results of investigations confirm the occurrence of one phase transition at $T_0 = 150 \pm 2 \text{ K}$. The integral parameters of the phase transition (enthalpy and entropy variations) determined by integration of the corresponding functions are $\Delta H = \int \Delta C_p dT = 275 \text{ J mol}^{-1}$ and $\Delta S = \int (\Delta C_p/T) dT = 1.8 \text{ J (mol K)}^{-1}$.

At the second stage, we carried out high-precision adiabatic calorimetry investigations on a calorimeter whose construction was described in [17] together with a specific heat measurement technique. The measurements were performed in the temperature range of 78–300 K on a cylindrical tableted sample with a mass of 0.384 g, a diameter of $d = 8 \text{ mm}$, and a height of $h = 2 \text{ mm}$ formed from the powder prepared by grinding small single crystals.

Figure 1 shows the molar specific heat of the Rb_2TaF_7 crystal.

We observed one anomaly in the form of a peak with the maximum at a temperature of $T_0 = 147.9 \pm 0.5 \text{ K}$, which was taken as the structural transformation temperature. The dashed line in the region of phase transition shows the lattice specific heat obtained by interpolation of the $C_p(T)$ data above and below T_0 using the Debye and Einstein functions. As a result, we refined the enthalpy and entropy of the phase transition as $\Delta H = 390 \pm 30 \text{ J mol}^{-1}$ and $\Delta S =$

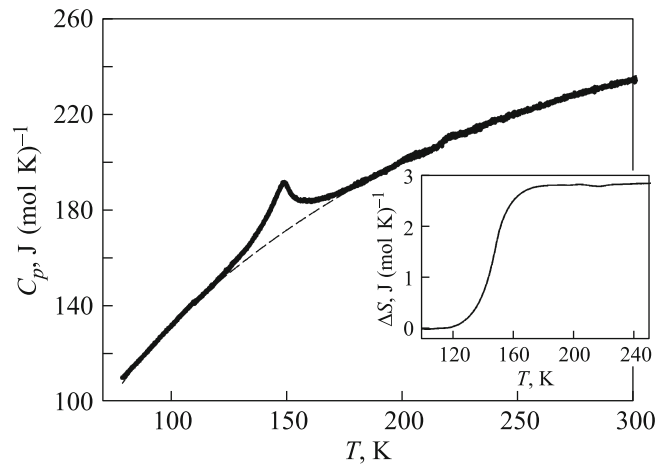


Fig. 1. Temperature dependences of the molar specific heat of Rb_2TaF_7 in a wide temperature range and anomalous entropy related to the phase transition (inset). The dashed line shows the lattice specific heat.

$2.6 \pm 0.2 \text{ J (mol K)}^{-1}$, respectively. Both integral parameters were found to be higher than those determined by the DSM method due to the higher sensitivity of the adiabatic calorimeter.

The dilatometric study was carried out on the sample used in the calorimetric measurements. The experiments on determination of the temperature dependence of the linear strain $\Delta L/L$ and linear thermal expansion coefficient α were conducted on a Netzsch DIL-402C induction dilatometer in the dry gas helium flow. The sample heating rate in the temperature range of 105–400 K changed from 2 to 4 K min^{-1} . The fused quartz reference was used for calibration and taking into account the expansion of the measuring system. The data obtained in several measurement series were consistent within 2–3%.

Figure 2 shows temperature dependences $\Delta L/L(T)$ and $\alpha(T)$ measured in the heating mode.

As in the calorimetric experiments, we observed one anomaly. The temperature of the $\alpha(T)$ peak maximum $T_0 = 145 \pm 1 \text{ K}$ taken as a phase transition temperature agrees satisfactorily with the T_0 value determined in the specific heat measurements. The inset in Fig. 2a shows the behavior of the anomalous portion of the linear strain $(\Delta L/L)_{an}$. It can be seen that the change in the sample length as a result of the phase transition is observed at temperatures up to 100 K and amounts to $\sim 0.1\%$

The polarization-optical study and birefringence measurements of the Rb_2TaF_7 crystal were performed on very thin ($d = 43 \mu\text{m}$) growth plates with the (001) $_T$ orientation on an Axioskop-40 microscope and Linkam LTS 350 temperature chamber. The accuracy of measurements of the birefringence absolute values Δn_c by the Berek compensator (Leica) method on a

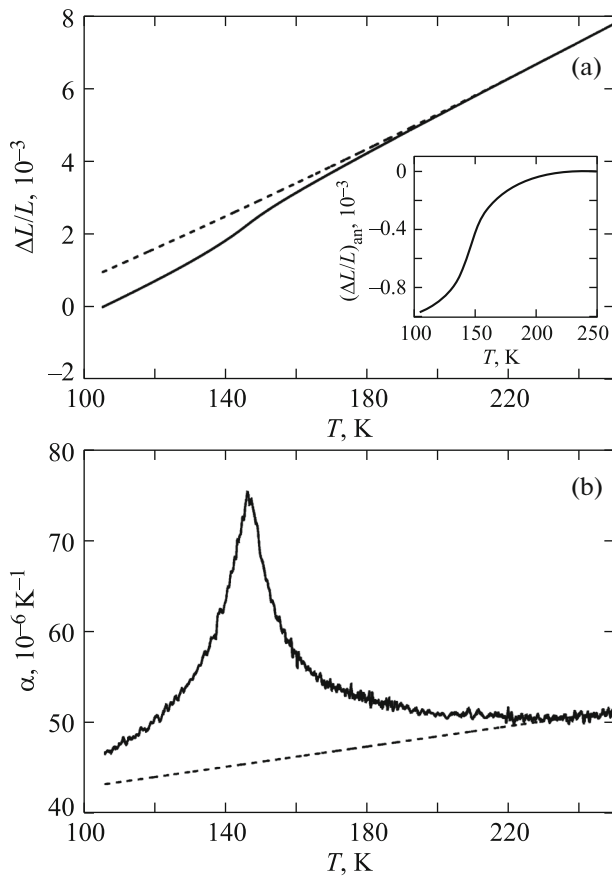


Fig. 2. Temperature dependences of (a) the linear strain, (inset) its anomalous component, and (b) linear thermal expansion coefficients. The dashed line shows the lattice contribution.

thin plate was low (± 0.0001), while the sensitivity to the change in $\Delta n_c(T)$ is ± 0.00001 .

At room temperature, the sample is nearly isotropic in accordance with the tetragonal symmetry. Upon cooling near $T_0 \sim 140$ K, the optical anisotropy and very fine strip twinning structure with the boundaries along $[100]$ appear in the microscope field. The total extinction of the plate occurs along $[110]$ (Fig. 3) and does not change with a further decrease in temperature. Thus, at the phase transition, the crystal syngony lowers from tetragonal to rhombic. The experimental geometry indicates that the crystals lose the $(100)_T$ symmetry elements and the unit cell axes of the low-temperature phase form along $[110]_R$ (base-centered cell C). Thus, our observations confirm the conclusions made in [15] concerning the symmetry variation at the phase transition in the Rb_2TaF_7 crystal: $G_2(Cmma) \leftrightarrow G_1(P4/nmm)$. The picture of twinning in the rubidium compound is drastically different from the picture observed earlier for $(\text{NH}_4)_2\text{TaF}_7$ [16], where the unit cell in the rhombic phase remains primitive: $G_1(P4/nmm) \leftrightarrow G_2(Pmmn) \leftrightarrow G_3$ (tetragonal phase).

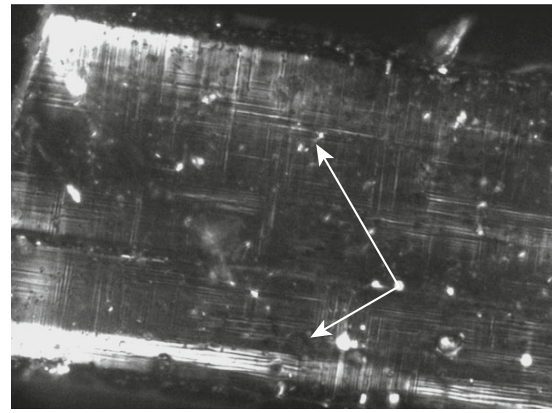


Fig. 3. Twinning of the low-temperature phase in $(001)_T$ growth plates of the Rb_2TaF_7 crystal.

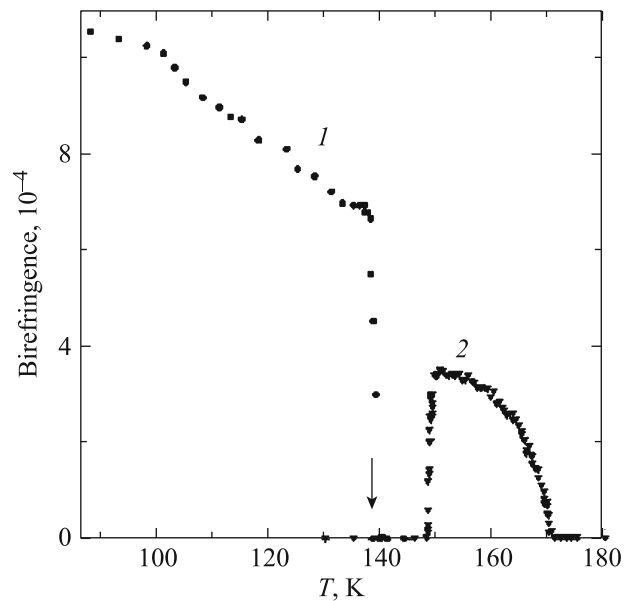


Fig. 4. Temperature dependences of birefringence $\Delta n_c(T)$ in (1) the Rb_2TaF_7 and (2) $(\text{NH}_4)_2\text{TaF}_7$ crystals [16].

The birefringence measurements were performed in the quasi-static mode upon heating and cooling. The temperature dependence $\Delta n_c(T)$ is presented in Fig. 4. The birefringence arises stepwise upon cooling and vanishes upon heating to temperatures of $T_0 = 138\text{--}139$ K. For comparison, Fig. 4 shows the birefringence in the native compound $(\text{NH}_4)_2\text{TaF}_7$ [16]. It can be seen that substitution of rubidium for ammonium led to a significant decrease in the phase transition temperature and to a slight increase in the birefringence. In addition, the transition to the rhombic phase of the rubidium compound has the pronounced features of the first-order transition, which is indicated by the $\Delta n_c(T)$ jump and a small temperature hysteresis of $\delta T_0 = 0.5$ K. In the ammonium compound, the tran-

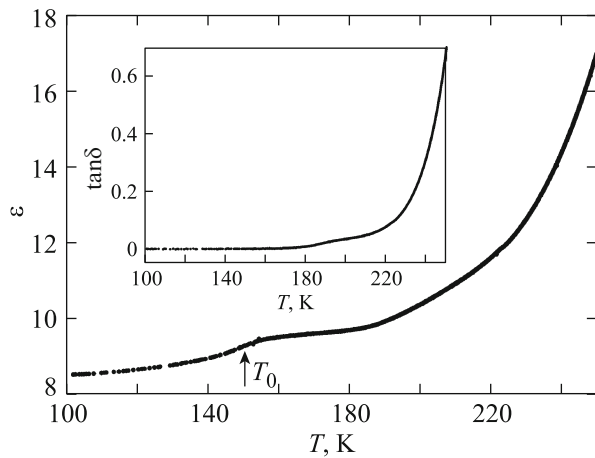


Fig. 5. Temperature dependences of permittivity ϵ and dissipation factor $\tan\delta$ (inset) of Rb_2TaF_7 at a frequency of 1 kHz.

sition $G_1(P4/nmm) \leftrightarrow G_2(Pmmn)$ is second-order. The observed differences between the behaviors of optical properties of Rb_2TaF_7 and $(\text{NH}_4)_2\text{TaF}_7$ are most likely caused by the different rhombic phase symmetries of the crystals.

Although the cation substitution was not accompanied by the phase syngony change below T_0 , which, in addition, remained ferroelastic, we carried out the permittivity investigation. The measurements were performed on a pseudo-ceramic sample used in the thermal property investigations. Silver electrodes were formed by vacuum sputtering. The possibility of examination of the dielectric properties of such samples was demonstrated by comparing the $\epsilon(T)$ data obtained on single-crystal plates and pseudo-ceramic samples of oxifluorides [18].

Figure 5 shows the temperature dependence of the permittivity, where one can observe the anomalous behavior in the form of a small fuzzy step at 140–160 K. Such a behavior of ϵ indicates that the Rb_2TaF_7 compound undergoes the nonferroelectric phase transition. The $\epsilon(T)$ inflection point is located near 150 K, which is in satisfactory agreement with the structural transformation temperature established in other experiments. The temperature dependence of the dissipation factor (inset in Fig. 5) also contains a hillock anomaly at a temperature of ~ 190 K, i.e., significantly above T_0 . The difference between the temperatures of the $\epsilon(T)$ and $\tan\delta(T)$ features is most probably explained by the fact that the change in the specific heat of the sample is related to the change in its sizes at the phase transition, while the dielectric loss are related, in particular, to the relaxation processes. The similar difference between the special temperatures was observed for $(\text{NH}_4)_2\text{TaF}_7$ [16].

3. RESULTS AND DISCUSSION

The complex investigations of some physical properties in the temperature range of 78–400 K showed that Rb_2TaF_7 does not undergo phase transitions, except for the transition $P4/nmm \rightarrow Cmma$ observed in [15]. The behaviors of twinning, birefringence, and permittivity of this fluoride are analogous to the behavior of the corresponding characteristics of $(\text{NH}_4)_2\text{TaF}_7$ established in [16], which is indicative of the ferroelectric state preservation in the Rb_2TaF_7 rhombic phase despite the change of the primitive cell for the base-centered one. At the same time, the cation substitution of rubidium for ammonium broadens the temperature region of stability of the initial tetragonal phase via lowering the structural transformation temperature.

The small entropy value ($\Delta S_0 \approx 0.3 R \ll R \ln 2$) suggests the absence of pronounced ordering of structural elements in Rb_2TaF_7 at the phase transition. In ammonium fluoride, the total entropy change related to the two sequential structural transformations was larger: $\Sigma \Delta S = \Delta S_1 + \Delta S_2 \approx 0.7 R \approx R \ln 2$ [16]. It follows from the behavior of specific heat and thermal expansion of $(\text{NH}_4)_2\text{TaF}_7$ that the anomalous contributions caused by the pronounced first-order transition between the rhombic $Pmmn$ and low-temperature tetragonal phases are imposed on the descending anomalous branches of $\Delta C_p(T)$ and $\Delta\alpha(T)$ below T_1 . Subtracting the entropy change $\Delta S_2 \approx 0.2 R$ related to the structural transformation at T_2 from $\Sigma \Delta S$, we obtain that the entropy of the transition $P4/nmm \leftrightarrow Pmmn$ is $\Delta S_1 \approx 0.5 R$.

In order to discuss the mechanism of structural distortions caused by the phase transitions, it is necessary to jointly analyze the features of entropy parameters and structural data on thermal parameters of critical atoms and/or ionic groups in the initial and distorted phases. For $(\text{NH}_4)_2\text{TaF}_7$, such structural data are missing. The models of the $P4/nmm$ and $Cmma$ phases structures in Rb_2TaF_7 based on the X-ray data for single crystals were proposed in [15]. The coordination anion polyhedron $[\text{TaF}_7]$ is a multicapped trigonal prism. In the $P4/nmm$ phase, the F1 atom lying on the fourth-order axis and four equatorial F2 atoms lying in the plane perpendicular to this axis are ordered. Two F3 atoms are dynamically disordered over four crystallographic positions upon rotation around the c axis. Thus, the seven-coordinate polyhedron $[\text{TaF}_7]$ is disordered and has two orientations relative to the fourth-order local axis. In the case of the fully ordered polyhedra (fluorine atoms) in the $Cmma$ phase, the entropy change could be $\Delta S_0 = 0.71 R = R \ln 2$. However, as was established in [15], after the transition the fluorine polyhedron remains disordered, but the heat parameters of fluorine atoms significantly decrease. This circumstance agrees satisfactorily with the small transition entropy $\Delta S_0 \approx 0.3 R \ll R \ln 2$, which is pro-

portional to the anharmonicity parameter $\delta = \langle \bar{x} \rangle^2 / a^2$, which relates the amplitude of oscillations of the critical atomic (ionic) parameter \bar{x} to the average interatomic distance a [19].

It should be noted that the oscillations of one of two nonequivalent Rb atoms are coordinated with the motion of disordered fluorine atoms and, thus, are also brightly anisotropic. We can assume with great confidence that in the fluoride $(\text{NH}_4)_2\text{TaF}_7$, the oscillations of the tetrahedral ion NH_4^+ occupying the corresponding crystallographic position can be more anharmonic than those typical of the spherical Rb atom and the transition at T_1 leads to the additional contribution to the entropy. In addition, it is obvious that the low-temperature transition to the tetragonal phase in $(\text{NH}_4)_2\text{TaF}_7$, which does not occur in Rb_2TaF_7 , is most likely associated with the change in the motion of an ammonium cation.

The absolute values of the linear thermal expansion coefficient of the Rb_2TaF_7 and $(\text{NH}_4)_2\text{TaF}_7$ crystals [16] far from the temperatures of structural transformations ($T = 240$ K, $\alpha \approx 5 \times 10^{-5}$ K $^{-1}$) almost coincide. However, in the region of the transition between the tetragonal phase $P4/nmm$ and rhombic phases $Cmma$ and $Pmnm$, the anomalous behaviors of $\Delta L/L$ and α are essentially different. In the ammonium crystal, the anomalous contribution to the bulk thermal expansion coefficient ($\beta = 3\alpha$ for a ceramic sample) has the negative sign, i.e., $\Delta\beta = \beta - \beta_{\text{lat}} < 0$, where β_{lat} is the lattice contribution [16]. Therefore, in the framework of the Ehrenfest equation [20], the baric coefficient, which characterizes the shift of the transition temperature T_1 under pressure, is also negative: $dT_1/dp = T_1(\Delta\beta/\Delta C_p) = -110$ K GPa $^{-1}$. For rubidium fluoride, we have $\Delta\beta > 0$ (Fig. 2b), which leads to an increase in the transition temperature under pressure. The calculation using the Ehrenfest equation with regard to the data on the specific heat jumps $\Delta C_p = 21$ J (mol K) $^{-1}$ and bulk expansion coefficient $\Delta\beta = 75$ K $^{-1}$ yields $dT_0/dp = 57$ K GPa $^{-1}$ for Rb_2TaF_7 . Analysis of the dependences of the thermal expansion coefficient and specific heat using the Pippard's equation allowed us to establish the linear dependence of $\beta(T)$ on $C_p(T)$ in the range of $\sim(T_0 - 6)$ K, according to which the baric coefficient is $dT_0/dp = 32$ K GPa $^{-1}$. The significant difference between the dT_0/dp values for Rb_2TaF_7 determined from the comparison of the anomalous $\Delta\beta$ and ΔC_p values at the transition point and dependences of the total $\beta(T)$ and $C_p(T)$ values can be explained by the different degrees of spread of the corresponding functions obtained in the experiments on quasi-ceramic samples at different temperature variation rates in the specific heat and thermal expansion measurements.

The different signs of the baric coefficients at the phase transition $P4/nmm \leftrightarrow (Cmma, Pmnm)$ in

Rb_2TaF_7 and $(\text{NH}_4)_2\text{TaF}_7$ can be explained considering the change in the linear and bulk parameters of the unit cell as a result of the cation substitution of rubidium for ammonium. Although the Rb ionic radius is larger than the radius of the cation group NH_4 , regardless of the number of nearest neighbors, the volume of the $P4/nmm$ rubidium unit cell (371.06 Å 3 [15]) appeared smaller than the volume of $(\text{NH}_4)_2\text{TaF}_7$ (371.30 Å 3 [16]). This is explained by the fact that the change in the chemical pressure as a result of the substitution of rubidium for ammonium appeared anisotropic, which is indicated by an increase in the parameters a and b by 0.29% and a decrease in the parameter c by 0.64%, which led to a decrease in the volume.

4. CONCLUSIONS

Study of the thermal, optical, and dielectric properties of Rb_2TaF_7 and their comparison with the previously investigated properties of $(\text{NH}_4)_2\text{TaF}_7$ [16] showed that substitution of spherical rubidium for tetrahedral ammonium cations results in the following.

The phase transition $P4/nmm \leftrightarrow Cmma$ in Rb_2TaF_7 established in [15] is ferroelastic and unrelated to the occurrence of the ferroelectric state.

According to the phase transition entropy $\Delta S_0 \approx 0.3R$, the pronounced ordering of structural elements does not occur, which agrees satisfactorily with the structural models of the initial and distorted phases.

The chemical pressure variation by means of the cation substitution was found to be anisotropic and leads to an increase in the parameters a and b and a significant decrease in the parameter c . This, in turn, changes the signs of the anomalous thermal expansion coefficients and baric coefficient dT/dp : in contrast to $(\text{NH}_4)_2\text{TaF}_7$, for which $dT/dp < 0$, the temperature of the phase transition in Rb_2TaF_7 increases with the hydrostatic pressure.

ACKNOWLEDGMENTS

The reported study was funded by the Russian Foundation for Basic Research, Government of Krasnoyarsk Territory, Krasnoyarsk Region Science and Technology Support Fund to the research project no. 16-42-243001.

REFERENCES

1. A. Tressaud, *Functionalized Inorganic Fluorides* (Wiley-Blackwell, Chichester, 2010).
2. M. Leblanc, V. Maisonneuve, and A. Tressaud, *Chem. Rev.* **115**, 1191 (2015).
3. I. Flerov, M. Gorev, K. Aleksandrov, A. Tressaud, J. Grannec, and M. Couzi, *Mater. Sci. Eng., R* **24**, 81 (1998).
4. I. N. Flerov, M. V. Gorev, M. S. Molokeev, and N. M. Laptash, in *Photonic and Electronic Properties of*

- Fluoride Materials*, Ed. by A. Tressaud and K. Poepelmeier (Elsevier, Amsterdam, 2016), Chap. 16.
5. I. N. Flerov, M. V. Gorev, A. Tressaud, and N. M. Laptash, *Crystallogr. Rep.* **56** (1), 9 (2011).
 6. E. C. Reynhardt, J. C. Pratt, A. Watton, and H. E. Petch, *J. Phys. C: Solid State Phys.* **14**, 4701 (1981).
 7. R. B. English, A. M. Heyns, and E. C. Reynhardt, *J. Phys. C: Solid State Phys.* **16**, 829 (1983).
 8. L.-S. Du, R. W. Schurko, K. H. Lim, and C. P. Grey, *J. Phys. Chem. A* **105**, 760 (2001).
 9. V. D. Fokina, M. V. Gorev, E. V. Bogdanov, E. I. Pogoreltsev, I. N. Flerov, and N. M. Laptash, *J. Fluor. Chem.* **154**, 1 (2013).
 10. A. M. Rodriguez, M. C. Caracoche, J. A. Martinez, and A. R. Lopez Garcia, *Hyperfine Interact.* **30**, 277 (1986).
 11. V. D. Fokina, I. N. Flerov, M. V. Gorev, E. V. Bogdanov, A. F. Bovina, and N. M. Laptash, *Phys. Solid State* **49** (8), 1548 (2007).
 12. V. D. Fokina, A. F. Bovina, E. V. Bogdanov, E. I. Pogoreltsev, N. M. Laptash, M. V. Gorev, and I. N. Flerov, *Phys. Solid State* **53** (10), 2147 (2011).
 13. I. N. Flerov, I. N. Gorev, V. D. Fokina, A. F. Bovina, E. V. Bogdanov, E. I. Pogoreltsev, and N. M. Laptash, *J. Fluorine Chem.* **132**, 713 (2011).
 14. W. Weber and E. Schweda, *Mater. Sci. Forum* **228**, 353 (1996).
 15. N. M. Laptash, A. A. Udovenko, and T. B. Emelina, *J. Fluorine Chem.* **132**, 1152 (2011).
 16. E. I. Pogoreltsev, S. V. Mel'nikova, A. V. Kartashev, M. S. Molokeev, M. V. Gorev, I. N. Flerov, and N. M. Laptash, *Phys. Solid State* **55** (3), 611 (2013).
 17. V. S. Bondarev, A. V. Kartashev, A. G. Kozlov, I. Ya. Makievskii, I. N. Flerov, and M. V. Gorev, Preprint No. 829F, IF SO RAN (Kirensky Institute of Physics, Siberian Branch of the Russian Academy of Sciences, Krasnoyarsk, 2005).
 18. I. N. Flerov, V. D. Fokina, A. F. Bovina, E. V. Bogdanov, M. S. Molokeev, A. G. Kocharova, E. I. Pogoreltsev, and N. M. Laptash, *Phys. Solid State* **50** (3), 515 (2008).
 19. V. G. Vaks, *Introduction to the Microscopic Theory of Ferroelectrics* (Nauka, Moscow, 1973) [in Russian].
 20. L. D. Landau and E. M. Lifshitz, *Course of Theoretical Physics, Vol. 5: Statistical Physics, Part 1* (Nauka, Moscow, 1964, Butterworth-Heinemann, Oxford, 1980).

Translated by E. Bondareva